Proceedings of the 2020 Design of Medical Devices Conference
DMD2020
April 6, 7-9, 2020, Minneapolis, MN, USA

DMD2020-9050

SOLID FIBER INSIDE CAPILLARY AND MODIFIED FUSION-SPLICED FIBER OPTIC MICRONEEDLE DEVICES

Jason N. Mehta[1], Christopher G. Rylander, PhD[1]
[1] Walker Department of Mechanical Engineering, The University of Texas at Austin
Austin, TX, USA

ABSTRACT

Clinical treatment of Glioblastoma Multiforme (GBM) is generally ineffective in increasing patient survival. Convection-enhanced delivery (CED) is an alternative, investigative therapy in which a small caliber catheter is placed directly into the brain parenchyma. However, standard CED drug delivery techniques are unable to reach the entirety of the brain tumor, attributing to the failure of Phase III clinical trials. Fiber optic microneedle devices (FMDs), capable of simultaneous fluid and laser energy delivery, have shown potential to increase the drug dispersal volume when compared to fluid only devices. Previously described FMDs have had low laser transmission efficiency. In this work, we present two FMD manufacturing methods, a solid fiber inside capillary (SFIC) FMD and a modified fusion spliced (FS) FMD. Transmission efficiency of the two proposed FMDs were measured using a 1064 nm laser and an integrating sphere detector with air, deionized water, and black ink inside of the bore of the FMDs. The transmission efficiency of the FS FMD was between 45 and 127% larger than that of previously reported FS FMDs. Additionally, the transmission efficiency of the SFIC was significantly higher than the FS FMD ($p \leq 0.04$ for all groups). However, the SFIC FMDs suffered catastrophic fracture failure at bend radii smaller than the manufacture specification, likely due to scribing of the capillary during the FMD fabrication process. Modifying FS FMDs appears to be the preferred fabrication method providing improved light transmission efficiency and mechanical strength on par with the capillary manufacturer's specifications.

1. INTRODUCTION

Glioblastoma Multiforme (GBM) is an extremely aggressive and infiltrative brain tumor with invisible margins typically extending centimeters from the MRI enhancing portion of the tumor [1]. Systemic chemotherapeutic treatment of GBM is complicated by the presence of the blood brain barrier (BBB) and the blood brain tumor barrier (BBTB) making systemic transport of large macromolecule drugs infeasible. The BBB and BBTB can be bypassed with the use of convection-enhanced delivery (CED). CED uses pressure driven loco-regional drug delivery in order to deliver large infusion payloads directly to the brain parenchyma [2, 3]. However, a retrospective study of Phase III (PRECISE) clinical trials concluded that poor drug distribution from off-label use of catheters could be responsible for the poor survival rates reported in the trial [4].

Fiber optic microneedle devices (FMDs) were previously developed to increase drug distribution during CED treatment [5]. FMDs utilize simultaneous fluid and laser energy co-delivery to increase the volumetric dispersal (V_d) of fluid between 60 and 80% in a healthy rodent model [6]. FMDs were manufactured either by gluing a standard solid core step-index fiber to the outer wall of a fused silica capillary tube [5, 7] or by fusion splicing a solid core step-index fiber to the annular wall of a light guiding capillary tube [6, 8]. The glued FMDs could delaminate during insertion and rely on off-axis light delivery which could be partially blocked by the capillary resulting in thermal degradation of the glue. On the other hand, fusion spliced FMDs allow for coaxial delivery of light; however, reported light coupling efficiency ranges between 30 and 55% [8, 9]. The low efficiency of the spliced FMDs could result in excessive heating at the splice location resulting in splice degradation, especially with CED treatments typically lasting several hours to several days [10]. In this study, we designed and tested two alternatives aimed at improving light guiding efficiency: 1) utilizing a solid fiber inside of a capillary tube (SFIC) FMD and 2) an improved fusion splicing technique (FS) FMD.

2. METHODS

[1] Contact author: cgr@austin.utexas.edu.

2.1 Design of Solid Fiber Inside Capillary (SFIC) FMD

Solid fiber inside capillary (SFIC) FMDs were fabricated by placing a solid core step-index fiber (100 µm core/ 110 µm cladding/ 130 µm buffer, ASF100/110/130T, Fiberguide Industries, Inc., Sterling, NJ) through the bore of a thin walled capillary tube (250 µm ID/ 375 µm OD, TSP250350, GS-Tek, Newark, DE). First, the capillary tubing is converted into a needle capable of dispensing fluid. The capillary tubing is cleaved from the spool, and each of the end faces are manually polished flat using polishing paper of sequentially decreasing grit sizes (30 µm to 1 µm). The capillary tubes are then glued into 22 gauge plastic dispensing needles using a medical grade epoxy (EA M-31CL, Henkel Corporation, Westlake, OH). Approximately 1 cm of the solid fiber's buffer is stripped using a warm sulfuric acid bath, the stripped end of the fiber is cleaved flat and inserted through the bore of the capillary tube such that the solid fiber terminates just beyond the termination of the needle, as shown in Fig. 1A. A luer lock t-connector is then placed over the fiber and connected to the needle via the mechanical luer lock. The fiber end of the luer connector is closed with medical grade UV cure acrylic (AA 3926, Henkel Corporation, Westlake, OH), with the open end of the t-connector allowing delivery of fluid through the FMD, as shown in Fig. 1B. A 2.5 mm ceramic ferrule is then attached to the proximal end of the solid fiber in order to allow coupling to a laser source.

In order to allow repeatable attachment and detachment of the SFIC FMD to the laser without requiring realignment for each prototype, the SFIC FMDs were designed to attach to a patch cable terminated with a 2.5 mm ceramic ferrule. A 50 µm core diameter was chosen for the patch cable because the nonstandard size of the solid fiber (110 µm cladding diameter) allows for approximately 16 µm of core misalignment when terminated within a standard 126 µm inner diameter ferrule. While the 50 µm cable will result in under filling of the solid fiber, it will not cause as great a loss in optical power as that caused by the coupling of two misaligned fibers. The total theoretical power loss can be determined from the general loss equation shown in Equation 1:

$$L_{total} = \alpha L + L_c + L_s \qquad (2)$$

Where L_{total} is the total loss in dB, α is the fiber attenuation, L is the length of the fiber, L_c is the connector loss, and L_s is the splice loss.

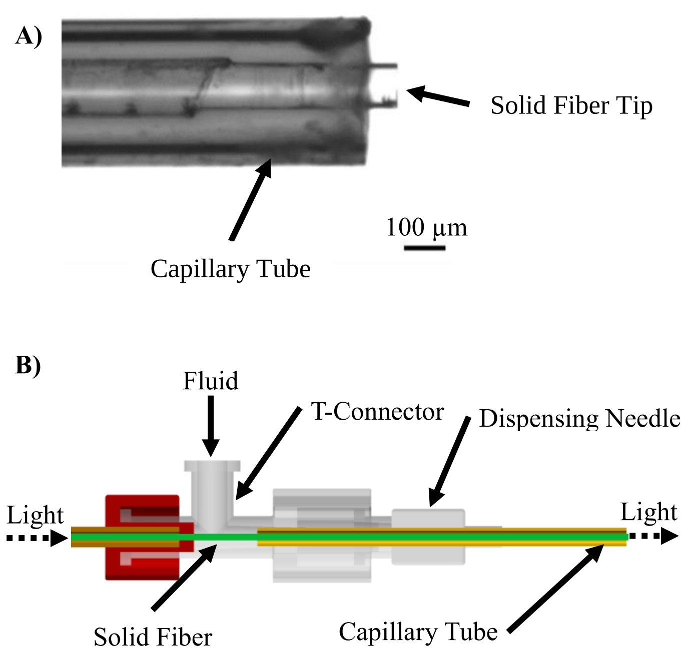

FIGURE 1: A) TIP OF SOLID FIBER INSIDE OF CAPILLARY (SFIC) FMD SHOWING SOLID FIBER PROTRUDING FROM THE CAPILLARY, **B)** CROSS-SECTIONAL SCHEMATIC ILLUSTRATION OF SFIC FMD (NOT TO SCALE).

2.2 Design of Fusion Spliced (FS) FMD

The preparation of the fusion spliced (FS) FMD is similar to that previously detailed [8]. Briefly, approximately 1 cm of the polyimide coating on both sides of a solid core step-index fiber (50 µm/ 70 µm/ 85 µm, FIP050070085, Polymicro Technologies, Phoenix, AZ) as well as 1 cm of the polyimide coating on one side of a light guiding capillary tube (150 µm ID/ 350 µm OD, LTSP150375, Polymicro Technologies, Phoenix, AZ) is stripped using a warm sulfuric acid bath. One end of the solid fiber is then terminated with a 2.5 mm ferrule and the other side of the fiber is cleaved flat. The light guiding capillary is polished flat using an electric end polisher (ULTRAPOL 1200, ULTRA TEC Manufacturing, Inc., Santa Ana, CA), using sequentially decreasing grit sizes from 30 µm to 1 µm.

The splicing instrumentation and parameters have been modified from previously reported FS FMD manufacturing techniques [8] to improve their light transmission. In order to splice the solid fiber with the light guiding capillary both fibers are placed into a fusion splicer (S178 LDF, Furukawa Electric Co., LTD, Tokyo, Japan). The splicer automatically aligns the fibers center to center, then the solid core fiber is manually moved by 110.8 µm using an electric linear stage such that the core of the solid fiber is aligned to the light guiding core of the capillary, as shown in Fig. 2. The splice is then created using a custom designed splicing protocol. Based on recommendations for splicing hollow core photonic crystal fibers (PCF) to solid core single mode fiber [11], the electrodes are biased by 10 µm toward the larger light guiding capillary so more energy would reach the capillary than would reach the solid fiber, reducing the chance of overheating the solid fiber. Additionally, a two-step arc duration was applied with the first step being 1 second long and the second step being 2 seconds long. Arc length was chosen according to results reported by Kato *et al.* in which arc lengths of longer than 1 second were found to increase tensile strength of fusion spliced single mode fibers [12]. The fist-step arc power was 40 AU and the second-step arc power ramped from 40 to 70 AU (power is a proprietary Furukawa unit). Further, the z-push distance was 20 µm, arc offset was -10 µm, and the gap offset was 5 µm. The theoretical efficiency of a spliced fiber, taking into account both the core diameter and axis offsets, but ignoring factors such as cleave quality, core non-circularity, dust

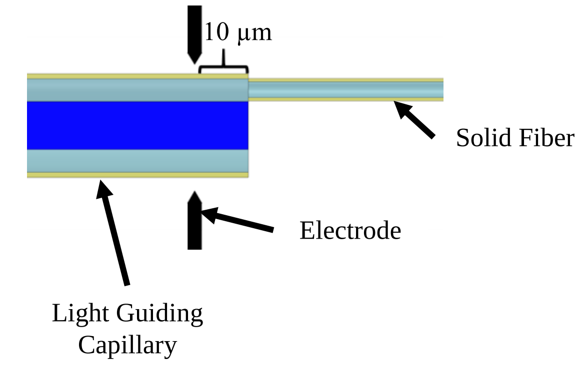

FIGURE 2: CROSS-SECTIONAL SCHEMATIC OF FUSION SPLICED (FS) FMD.

contamination, and insertion loss can be determined by Equation 2:

$$L_{splice} = -10\log\left[\left(\frac{2AB}{A^2+B^2}\right)^2 \exp\left(-\frac{2d^2}{A^2+B^2}\right)\right] \quad (2)$$

Where L_{splice} is the splice efficiency in dB, A is the mode field diameter of the solid fiber, B is the mode field diameter of the light guiding capillary, and d is the core offset between the solid fiber and the capillary.

After the splice is created, the splice junction is protected by fixing a larger capillary (450 µm ID, 670 µm OD, TSP450670, Polymicro Technologies, Phoenix, AZ)) tube over the junction with UV cure acrylic (AA 3926, Henkel Corporation, Westlake, OH). The entire spliced fiber is then inserted into a t-connector and UV cure acrylic is used to fix the spliced FMD into the connector, as shown in Fig. 3.

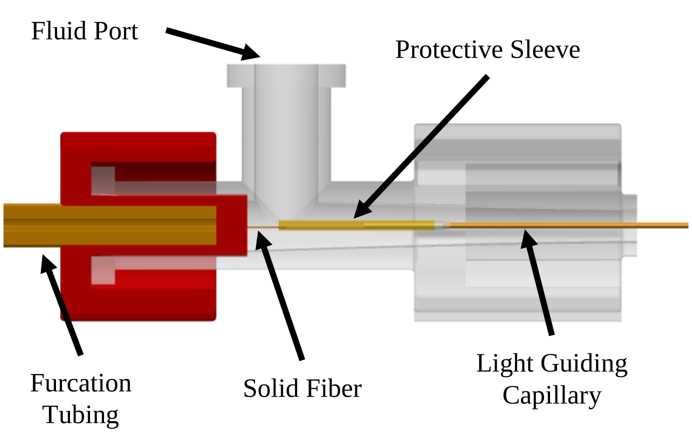

FIGURE 3: CROSS-SECTION OF FUSION SPLICED (FS) FMD AFTER ADDING A PROTECTIVE CAPILLARY SLEEVE OVER THE SPLICE JUNCTION AND ATTACHING TO A T-CONNECTOR.

2.3 Experimental FMD Light Transmission Efficiency Procedure

Due to the high penetration depth of near infrared light in both healthy [13] and tumorous [14] brain tissue, a 1000 mW 1064 nm diode pumped solid state laser (LRS-1064-PFM, Laserglow Technologies, Toronto, Ontario, Canada) was used to test the transmission efficiency of the two alternative FMD designs. The laser was connected to a patch cable (M14L02, Thorlabs Inc., Newton, New Jersey) which was modified to have a 2.5 mm ferrule at the emitting end of the cable. The ferrule was then connected to the corresponding 2.5 mm ferrule on the FMD using a ferrule mating sleeve (ADAF, Thorlabs Inc., Newton, NJ). A 100 mW output from the patch cable was created by an analog voltage output (NI9264/ NI USB-9162, National Instruments, Austin, TX) set in a custom LabView program. In order to differentiate between insertion loss and splice efficiency, the power of the solid core fibers for the FS FMDs were measured after fiber termination but before splicing, using an integrating sphere detector (918D-SL-OD1, Newport Corporation, Irvine, CA) connected to a power meter (Model 1931-C, Newport Corporation, Irvine, CA) which recorded data directly to the LabView program. The FS FMD was then spliced and the emitting end of the FMD was manually polished flat using sequentially decreasing grit polishing paper from 30 µm to 1 µm in order to ensure a smooth end face for the emitting side of the FMD. Three FMDs of each design were fabricated for power transmission testing. Power was measured in the same manner for both the SFIC and the FS FMDs. First, the emitting end of the FMD was inserted into a bare fiber terminator which was inserted into the integrating sphere detector. The bare fiber terminator ensured that the FMDs were consistently placed in the same position inside of the detector. The power was measured initially with just air in the bore of the FMD, then deionized (DI) water was flushed through the FMD and power was measured again, finally, the DI water was removed and black ink (Speedball Super Black India Ink, Speedball, Statesville, NC) was used to flush the FMD, and power was measured once more. For each measurement, the laser emitted light for 10 minutes; however, in order to allow the laser power to stabilize, power was measured every second during the last 30 seconds of the measurement and averaged over the measurement period. At the conclusion of the experiment, the SFIC and FS FMDs were compared for different transmission efficiencies using a two sample t-test. Further, a paired t-test was used to compare the total efficiency (including both insertion loss and splice efficiency) with the splice efficiency. Finally, in order to test for potential cable and splice degradation over time, two more SFIC and FS FMDs were manufactured. The first of each FMD type was used to emit approximately 200 mW for 8 hours, and the second of each FMD type was used to emit 500 mW for 8 hours. Additionally, as a reference to the stability of the laser, the power output of a patch cable was also measured for 8 hours. Power was measured using a similar setup as before, with data being collected every minute for the full 8 hour test. An 8 hour test was chosen due to practical limitations of the experiment and an inability of the lasers to remain on outside of normal work hours.

3. RESULTS

3.1 Theoretical Efficiency

The length of the cable used for the SFIC FMD is around 2 m and the attenuation of fiber optic cables is on the order of dB per km, therefore the expected attenuation due to fiber length is negligible. The ferrule mating sleeve has a rated typical insertion loss of less than 1.0 dB, so the connector loss can be estimated at 1 dB. Lastly, the splice loss from the SFIC FMD is 0 dB since no splice was used in manufacturing the FMD. Using Equation 1, we can find a total anticipated loss of less than 1 dB which corresponds to an expected efficiency of greater than 89% for the SFIC FMD.

The FS FMD efficiency can be calculated in a similar way as the SFIC. The length of the fiber is again negligible, the connector loss will also be less than 1 dB, and the splice loss can be determined using Equation 2. We set mode field diameter of the solid fiber set to the core diameter of the solid fiber and the mode field diameter of the light guiding capillary to the core radius of the capillary (71.5 µm). Then two cases were analyzed: 1) where there is no core misalignment (d = 0 µm) and 2) where the core misalignment is determined as if the top edge of the solid fiber is aligned to the top edge of the light guiding capillary (16.75 µm). The first case yields a splice loss of 0.54 dB and the second case results in a splice loss of 0.86 dB. The splice efficiency of the FS FMD should be between 82 and 88%. Adding the 1 dB loss from the connector, the total efficiency for the FS FMD should be between 65 and 70%.

3.2 Experimental FMD Efficiency

The SFIC FMD had a significantly higher transmission efficiency with air, DI water, and black ink in the bore compared to the FS FMD ($p = 0.04$, $p = 0.04$, and $p = 0.003$ respectively). The average efficiency for SFIC FMD with air, DI water, and black ink in the bore was 95.1 ± 2.7%, 91.7 ± 8.5%, and 83.1 ± 10.8% respectively, whereas the efficiencies for the FS FMD were 79.6 ± 8.6%, 72.8 ± 6.8%, and 27.2 ± 10.2% respectively. Fig. 4A shows the total efficiency of both the SFIC and the FS FMDs. The difference in total efficiency compared to splice efficiency of the FS FMD was not significant with air and DI water in the bore of the needle ($p > 0.16$). However, there was a small, yet significant difference between efficiencies when black dye was in the bore of the FS FMD ($p = 0.03$). Fig. 4B shows the total efficiency as well as the splice efficiency plotted with the different media inside of the bore.

After 8 hour testing of each of the FMDs, both the SFIC and FS FMDs had greater efficiency deviation than the patch cable, as shown in Fig. 5. The average output of the 200 mW FS FMD was 193.8 ± 2.0 mW whereas the average output of the SFIC FMD was 202.9 ± 2.0 mW. The average output of the 500 mW FS FMD was 494.8 ± 8.1 mW and the average output of the 500 mW SFIC FMD was 508.9 ± 2.1 mW. The deviation from the average power of the FS 200 mW FMD was 5.1% compared to a deviation of 5.3% for the SFIC FMD. The deviation of the 500 mW spliced FMD was 8.2% compared to 2.3% for the SFIC FMD. The deviation of the patch cable over the 8 hour span was 2.1%.

4. DISCUSSION

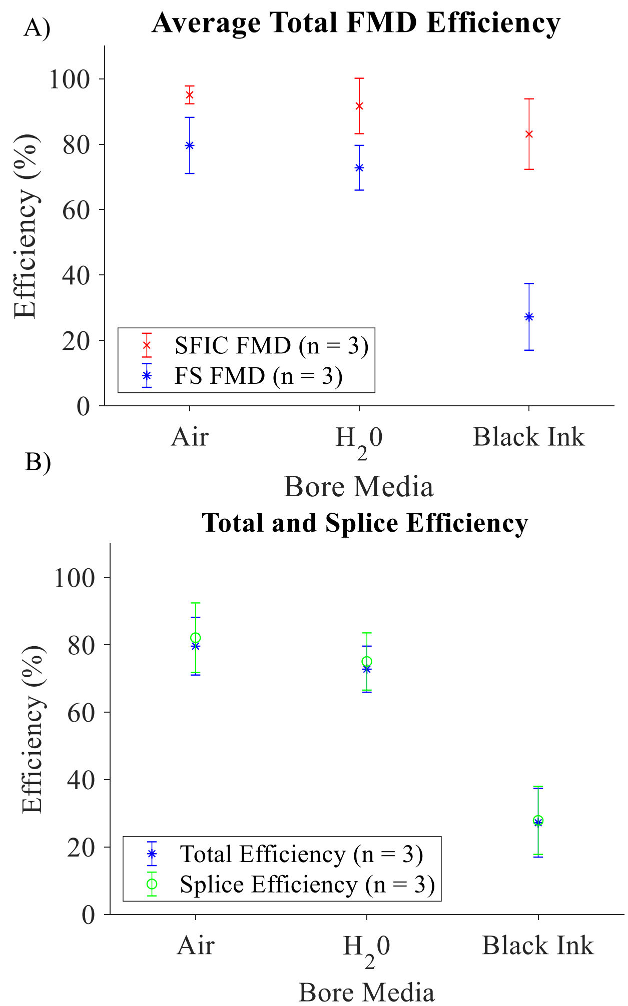

FIGURE 4: A) PLOT OF THE TRANSMISSION EFFICIENCY (%) DEPENDENCE ON THE MEDIA INSIDE OF THE BORE OF THE FMD FOR BOTH THE SOLID FIBER INSIDE OF CAPILLARY (SFIC) AND THE FUSION SPLICED (FS) FMDS, **B)** PLOT OF THE TRANSMISSION EFFICIENCY OF THE FS FMD WITH DIFFERENT BORE MEDIA WHEN TOTAL EFFICIENCY (INCLUDING INSERTION LOSS) AND SPLICE EFFICIENCY ONLY ARE MEASURED.

The measured efficiency in air for the SFIC FMD was about 7% higher than the theoretical efficiency. The measured total efficiency for the FS FMD was between 14 and 20% higher than the theoretical total efficiency. Taking into account the SFIC FMD efficiency and the efficiency of the FS fiber before splicing the total connector loss was around 0.17 dB, which is much closer to manufacturer reported connector losses of other standard connectors that do not use a ferrule sleeve, suggesting that insertion loss caused by the ferrule sleeve adapter is much lower for the fiber size and wavelength used in this study compared with that used in the testing conducted by the manufacturer.

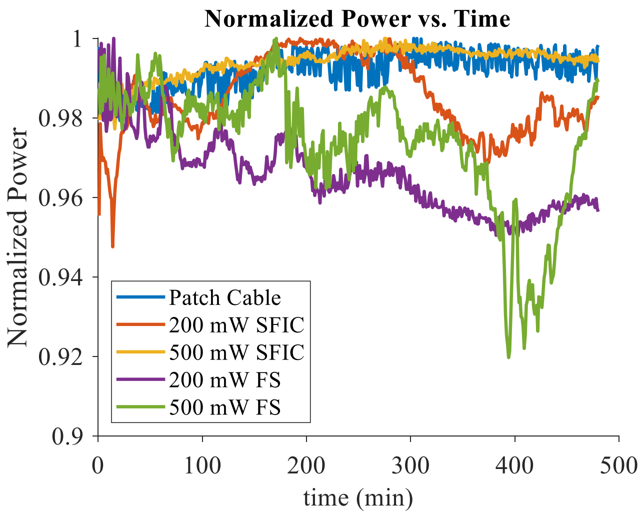

FIGURE 5: NORMALIZED POWER PLOTTED AGAINST TIME FOR THE PATCH CABLE, 200 MW SOLID FIBER INSIDE OF CAPILLARY (SFIC) FMD, 500 MW SFIC FMD, 200 MW FUSION SPLICED (FS) FMD, AND 500 MW FS FMD.

The splice efficiency was between 0.1% greater and 7% lower than the theoretical splice efficiency. The splice efficiency was likely on the low end of the theoretical calculations due to imperfect alignment between the two spliced components as well as slight angular misalignments between the two fibers caused by variations in the cleave and polishing angles.

The transmission efficiency of the fusion spliced FMD, with air through the bore was nearly 80% which is between a 45% and 127% improvement over previously published efficiencies [8, 9]. Additionally, since the transmission efficiency of both the FS and the SFIC FMDs do tend to have a larger deviation over 8 hours than just a patch cable, the discrepancy is likely not due to splice or fiber degradation, but more likely caused by the coupling of the patch cable to the respective FMDs. But, since the 500 mW FS FMD had a much larger deviation than any other group, some thermal degradation is likely occurring at high powers. It should also be noted that although we did not find significant reduction in power transmission after 8 hours, CED infusions can last as long as a few days [10]. While we do not anticipate the use of co-delivery for time periods exceeding 8 hours if it ever becomes necessary, longer duration testing should be conducted.

The transmission efficiency of the SFIC FMS was superior to that of the FS FMD, especially when an extremely light absorptive infusate, such as black dye is used. Since the SFIC FMD uses a standard step index fiber with cladding on the outside of the fiber, no absorption of light was expected along the axis of the FMD. However, the light guiding capillary does not have cladding along the inner diameter of the light guiding capillary, allowing light to be absorbed by the media inside of the bore. Therefore, in order to further assess the viability of FS FMDs exploration on the effects of specific drugs and light transmission as well as the effect of the heating on the potency of specific drugs should be studied.

While there are many benefits of using the SFIC two factors reduce its practical efficacy. First, adding the solid fiber (130 µm) to the bore of the capillary (250 µm ID) reduces the hydraulic diameter of the FMD by ~52%. Since the hydraulic resistance of laminar flow according to the Hagen-Poiseuille law is proportional to the diameter raised to the fourth power, significantly more pressure would be needed to create similar flow rates. Due to the low flowrates of between 0.5 and 10 µL/min [15] typically associated with CED, the SFIC FMD will likely not be flow rate limited as catheter internal diameters as low as 50 µm have been used previously [16]. However, the smaller hydraulic diameter of SFIC FMD will result in a larger infusion pressure than the FS FMD. Additionally, the SFIC FMDs are prone to breakage at bend radii of about 19.5 mm. The likely cause of failure is the manufacturing process where the solid fiber is inserted into the bore of the capillary tube, during this time, the solid fiber is permitted to contact the inner wall of the capillary which could cause scoring of the capillary tube. This scoring, if deep enough (approximately 1 µm) could allow the capillary to be easily cleaved. Fig. 6A, B, and C show images of potential scoring within the bore of the capillary as well as needle failure due to fracture.

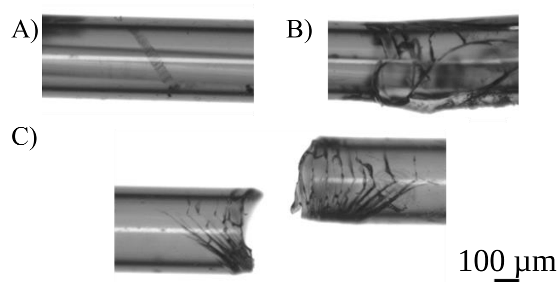

FIGURE 6: A) SCRIBING INSIDE OF CAPILLARY POSSIBLY CAUSED BY FIBER INSERTION, **B)** HEAVY CRACKING NEAR CAPILLARY FAILURE POINT, AND **C)** TWO HALVES OF CRACKED CAPILLARY.

4. CONCLUSION

We present two alternative designs and methods of FMD fabrication that can be used to improve light transmission efficiency compared to previously reported designs. The SFIC design has greater light transmission efficiency than the FS design; however, the FS design is advantageous due to its increased fluid conductance and greater mechanical strength. This improvement in efficiency allows for the co-delivery of both fluid and laser energy with a reduced worry of degradation of the device and excessive heating of the delivered infusate. Future work will focus on absorptivity of potential drugs for CED treatment as well as the interaction of the drug with the addition of thermal energy.

ACKNOWLEDGEMENTS

This research was funded by the National Insitutes of Health/ National Cancer Institute, grant number P01 CA207206-01.

CONFLICT OF INTEREST

The fiber optic microneedle device fabrication methods and applications are described in US Patent 10,220,124 issued on March 5, 2019 managed by the Virginia Tech Intellectual Properties (VTIP) Group. The NIH had no role in the design of the study; in the collection, analyses, or interpretation of data; in the writing of the manuscript, or in the decision to publish the results.

REFERENCES

[1] DeAngelis, L. M., 2001, "Brain Tumors," N Engl J Med, 344(2), pp. 114-123.
[2] Bobo, R. H., Laske, D. W., Akbasak, A., Morrison, P. F., Dedrick, R. L., and Oldfield, E. H., 1994, "Convection-enhanced delivery of macromolecules in the brain.," Proc Natl Acad Sci U S A, 91, pp. 2076-2080.
[3] Morrison, P. F., Laske, D. W., Bobo, H., Oldfield, E. H., and Dedrick, R. L., 1994, "High-flow microinfusion: tissue penetration and pharmacodynamics," Am J Physiol, 266(1 Pt 2), pp. R292-305.
[4] Sampson, J. H., Archer, G., Pedain, C., Wembacher-Schroder, E., Westphal, M., Kunwar, S., Vogelbaum, M. A., Coan, A., Herndon, J. E., Raghavan, R., Brady, M. L., Reardon, D. A., Friedman, A. H., Friedman, H. S., Rodriguez-Ponce, M. I., Chang, S. M., Mittermeyer, S., Croteau, D., Puri, R. K., and Investigators, P. T., 2010, "Poor drug distribution as a possible explanation for the results of the PRECISE trial," J Neurosurg, 113(2), pp. 301-309.
[5] Hood, R. L., Ecker, T., Andriani, R., Robertson, J., Rossmeisl, J., and Rylander, C. G., "Augmenting convection-enhanced delivery through simultaneous co-delivery of fluids and laser energy with a fiberoptic microneedle device," Proc. SPIE BiOS, International Society for Optics and Photonics, pp. 85760G-85760G.
[6] Hood, R. L., Andriani, R. T., Jr., Emch, S., Robertson, J. L., Rylander, C. G., and Rossmeisl, J. H., Jr., 2013, "Fiberoptic microneedle device facilitates volumetric infusate dispersion during convection-enhanced delivery in the brain," Lasers Surg Med, 45(7), pp. 418-426.
[7] Hood, R. L., Andriani, R. T., Ecker, T. E., Robertson, J. L., and Rylander, C. G., 2015, "Characterizing Thermal Augmentation of Convection-Enhanced Drug Delivery with the Fiberoptic Microneedle Device," Engineering, 1(3), pp. 344-350.
[8] Hood, R. L., Rossmeisl, J. H., Jr., Andriani, R. T., Jr., Wilkinson, A. R., Robertson, J. L., and Rylander, C. G., 2013, "Intracranial hyperthermia through local photothermal heating with a fiberoptic microneedle device," Lasers Surg Med, 45(3), pp. 167-174.
[9] Hood, R. L., 2013, "Development of a Fiberoptic Microneedle Device for Simultaneous Co-Delivery of Fluid Agents and Laser Light with Specific Applications in the Treatment of Brain and Bladder Cancers," Doctor of Philosophy, Virginia Polytechnic Institute and State University Blacksburg, Virginia.
[10] Vandergrift, W. A., Patel, S. J., Nicholas, J. S., and Varma, A. K., 2006, "Convection-enhanced delivery of immunotoxins and radioisotopes for treatment of malignant gliomas," Neurosurg Focus, 20(4), p. E13.
[11] 2009, "Splicing Single Mode PCFs," NKT Photonics Application Note, NKT Photonics, Birkerod, Denmark, p. 3.
[12] Kato, Y., Seikai, S., and Tateda, M., 1982, "Arc-fusion splicing of single-mode fibers. 1: Optimum splice conditions," Appl. Optics, 21(7), pp. 1332-1336.
[13] Svaasand, L. O., and Ellingsen, R., 1983, "Optical properties of human brain," Photochemistry and photobiology, 38(3), pp. 293-299.
[14] Svaasand, L. O., and Eixingsen, R., 1985, "Optical penetration in human intracranial tumors," Photochemistry and photobiology, 41(1), pp. 73-76.
[15] Kanner, A., 2007, "Convection-enhanced delivery high-grade gliomas," Current clinical oncology, pp. 303-314.
[16] Fernández, L. J., Altuna, A., Tijero, M., Gabriel, G., Villa, R., Rodríguez, M. J., Batlle, M., Vilares, R., Berganzo, J., and Blanco, F., 2009, "Study of functional viability of SU-8-based microneedles for neural applications," Journal of Micromechanics and Microengineering, 19(2), p. 025007.